Evaluating Voltage Notch Problems Arising from AC/DC Converter Operation

Reza Ghandehari, *Student Member, IEEE*, and Abbas Shoulaie

***Abstract*—This paper analyzes the voltage notches in ac/dc converters and the problems that they create. Voltage notch disturbs the voltage's waveform and excites the natural frequencies of the system. In some systems, these excisions create considerable high-frequency oscillations in the voltages of the converter and the adjacent buses; this can damage capacitor banks, create parallel resonance, and generate radio disturbances. This paper analyzes the effect of snubber circuits on the voltage oscillations that arise from commutation. It also presents the theoretical foundation and analytical derivation that are used to calculate notch depth and the frequency of oscillations. To achieve accurate and applicable results, various loads of the converter, the dc current ripple, and the characteristic impedance of the system are considered. Several experimental results are shown in order to illustrate the effects of changes in the system and converter parameters on the voltage waveform of the converter. Computer simulations and experimental results indicate the accuracy of the theoretical relations. The proposed equations make it possible to effectively study the harmonic and power quality in networks that include high-power converters.**

***Index Terms*—AC/DC converter, high-frequency oscillations, snubbers, voltage notch.**

I. Introduction

THE NUMBER and power ratings of ac/dc converters have continuously increased in power systems, and have become more effective on power quality indexes. Although harmonics are known as the most critical disturbance of converters and have been studied in many papers [1]–[7], voltage notches can considerably affect the voltages of converters and adjacent buses but have been considered less frequently [8].

Simultaneous conduction of switches in an ac/dc converter during the commutation period causes a two-phase short circuit via switching elements. The voltage loss that results from this short circuit in the converter voltages causes disturbances in the voltage waveform, which is called the *voltage notch*. These abrupt and regular changes in the voltage of the converter destroy the voltage sinusoidal waveform, which causes the excitation of the natural frequencies of the electrical network. Excitation of the system's natural frequencies via the voltage notch can generate noticeable oscillations in the voltage and the current characteristics of the converter [9]–[11]. These oscillations can cause some problems, such as damaged capacitor banks, parallel resonance, radio disturbances, and electronic device malfunction [8]–[10].

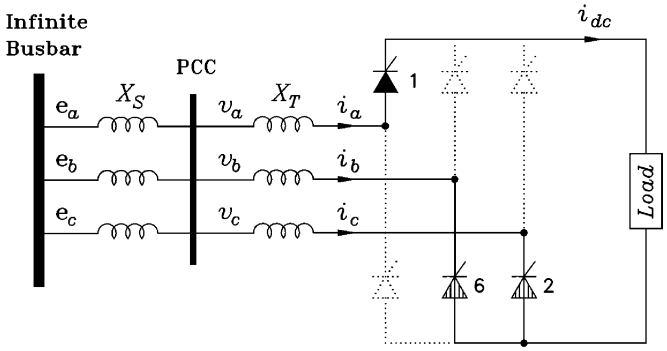

Fig. 1. Three-phase ac/dc converter during the third conduction period.

The frequency and magnitude of such oscillations depend on the circuitry structure of the network, the size of the system impedance as seen from the converter bus, and the size of the capacitor banks [8]. If the capacitor banks of the network are neglected, then the capacitors of the snubber circuits will produce some high-frequency oscillations in the voltage and current waveforms [12], [13].

The notch depth and area are proper indexes of the voltage notch phenomenon, which is noticeable in the study and investigation of power quality status. The depth value of the voltage notch and its area in the converter bus depends on the impedance value between the converter and the point of common coupling (PCC) (X_T), and on the system impedance, as seen from PCC (X_S) (see Fig. 1). Higher impedance between converter and PCC correlates to a lower value of voltage notch depth in that feeder, which improves the power quality [8]–[14]. Certain definitions and recommendations have been proposed regarding the allowable limits of notch indexes [15], [16].

This paper presents an accurate study of the theoretical and experimental aspects of the converter's voltage notch and its problems. First, the classical definitions and relations of the voltage notch are described. Snubber circuits are considered as one of the oscillations that create factors during the commutation period; next, their effects on converter voltage and current are examined. In the next step, these characteristics are obtained regarding the ripple of the converter's dc line current.

The effects of the network's capacitive elements, such as the capacitor banks, filters, and cables on the converter voltage and the current oscillations during and after commutation are explained. In each step, one of the conduction periods is

Manuscript received January 21, 2009; revised March 23, 2009. Current version published August 21, 2009. Recommended for publication by Associate Editor J. HR Enslin.

R. Ghandehari is with the Tehran Regional Electrical Company (TREC) Tehran 16846-13114, Iran, and also with the Electrical Engineering Department, Iran University of Science and Technology (IUST), Tehran 16846-13114, Iran (e-mail: r_ghandehari@iust.ac.ir).

A. Shoulaie is with the Electrical Engineering Department, Iran University of Science and Technology (IUST), Tehran, 16846-13114, Iran (e-mail: shoulaie@iust.ac.ir).

Color versions of one or more of the figures in this paper are available online at http://ieeexplore.ieee.org.

Digital Object Identifier 10.1109/TPEL.2009.2021058

TABLE I
TWELVE CONDUCTION PERIODS OF THE CONVERTER

Conduction period	1	2	3	4	5	6
Phase in upper layer of converter	$a\rightarrow c$	a	a	a	$b\rightarrow a$	b
Phase in lower layer of converter	b	b	$c\rightarrow b$	c	c	c
Conduction period	7	8	9	10	11	12
Phase in upper layer of converter	b	b	$c\rightarrow b$	c	c	c
Phase in lower layer of converter	$a\rightarrow c$	a	a	a	$b\rightarrow a$	b

discussed. The obtained results can be generalized to other conduction periods. Lastly, the experimental and simulation results are compared with the achieved analyses at different conditions.

II. CLASSICAL ANALYSIS OF VOLTAGE NOTCH

In general, for a six-pulse ac/dc converter analysis, 12 conduction periods are considered; six periods for a two-switch operation (complete conductance) and six periods for a three-switch operation (see Table I).

If the voltages of the converter bus are considered symmetrical, then the related time equations of the main bus voltage, based on the parameters presented in Fig. 1, are given by

$$\begin{aligned} e_a(t) &= V_m \,\mathrm{Sin}(\omega t) \\ e_b(t) &= V_m \,\mathrm{Sin}\left(\omega t - \frac{2\pi}{3}\right) \\ e_c(t) &= V_m \,\mathrm{Sin}\left(\omega t + \frac{2\pi}{3}\right). \end{aligned} \tag{1}$$

To analyze the voltage notch, it is sufficient to select one of the commutation periods in Table I, write the system equations, and then generalize the obtained relations to other periods. Considering that the unbalanced voltage in the process of analysis is simple, in order to avoid the complexity of relations, however, the three-phase voltages of system are considered to be balanced. In the first step, the dc current of the converter is supposed to be smooth, and the snubber circuits are neglected. According to Fig. 1, for example, in the third conduction period, the current equation of the commutation circuit is [13], [16]

$$L_c i_b\big|_{i_b=i_{dc}}^{i_b} - L_c i_c\big|_{i_b=0}^{i_{dc}-i_b} = \int_{(\alpha+\pi/2)}^{\omega t} \sqrt{3} V_m \,\mathrm{Sin}\left(\omega t - \frac{\pi}{2}\right) d\omega t. \tag{2}$$

Based on this equation, the current and voltage of phase "b" (i_b and v_b) and the voltage notch depth ($V_{dep(b)}$) are obtained as follows:

$$i_b(t) = \frac{\sqrt{3} V_m}{2 L_C \omega}[\mathrm{Cos}(\alpha) - \mathrm{Sin}(\omega t)] + i_{dc} \tag{3}$$

$$v_b(t) = V_m \,\mathrm{Sin}(\omega t - 2\pi/3) - \frac{L_S}{2(L_T + L_S)} \sqrt{3} V_m \,\mathrm{Cos}(\omega t) \tag{4}$$

$$V_{dep(b)} = \frac{L_S}{2(L_S + L_T)} \sqrt{3} V_m \,\mathrm{Cos}(\omega t)\Big|_{\omega t = \alpha + \pi/2}. \tag{5}$$

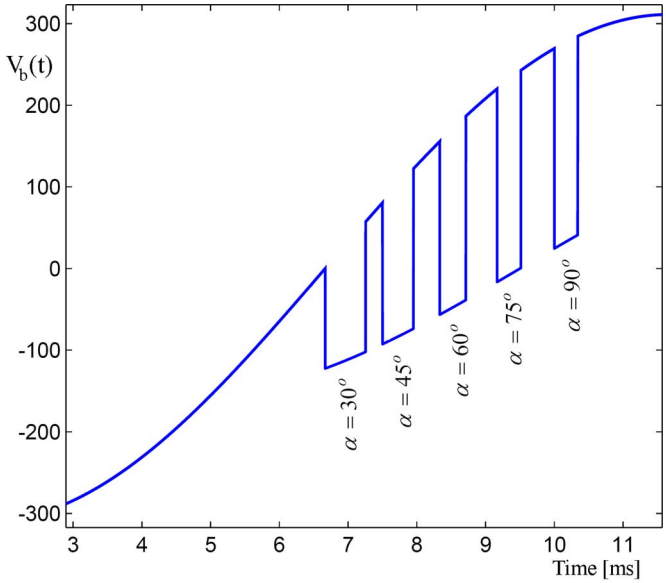

Fig. 2. Voltage notch with fire angle variations in the third conductance period.

TABLE II
SYSTEM PARAMETERS FOR AC/DC CONVERTER

Parameter	Value	Parameter	Value
$e_{(a,b,c)}$	220 V_{rms}	$X_{S(a,b,c)}$	0.314 Ω
f_s	50 Hz	$X_{T(a,b,c)}$	0.031 Ω
α	30 degree	R_L	5 Ω
$R_{S(a,b,c)}$	≈ 0 Ω	L_L	50 mH

Voltage notch depth depends on three factors: firing angle (α), system impedance as seen from PCC (X_S), and impedance between the PCC and the converter (X_T). In the third conductance period, with respect to (5), increasing the firing angle of the converter from 0° to 90°, as indicated in Fig. 2, increases the voltage notch depth. According to (5), the higher value of X_T/X_S causes the lower value of the notch depth in PCC voltages. To certify these equations, a converter with *RL* load and without capacitor banks at the system's buses is considered. The converter is simulated using the specifications given in Table II, while snubber circuits are neglected.

The results obtained from (4) and system simulation are compared in Fig. 3. The compatibility of the achieved waveforms with good precision indicates the accuracy of the obtained results regarding relative assumptions.

III. VOLTAGE NOTCH ANALYSIS USING SNUBBER CIRCUITS

In the analysis of voltage notches, particularly in systems with low short-circuit levels, it is impossible to neglect the effects of snubber circuits on the voltages and current characteristics of converters.

Fig. 4 shows an ac/dc converter during the first conduction period, where two phases "a" and "c" are in commutation at the upper switches of the converter and where phase "b" is in the complete conduction state at the lower switches. In this status, it

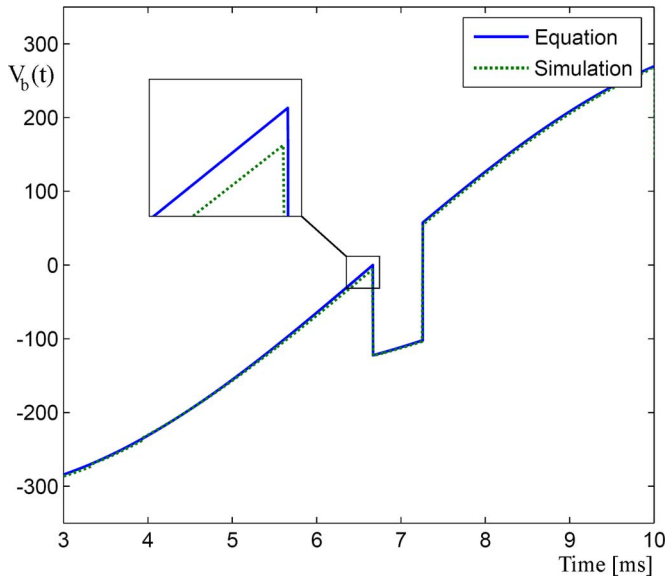

Fig. 3. Voltage notch on the voltage waveforms of converter bus.

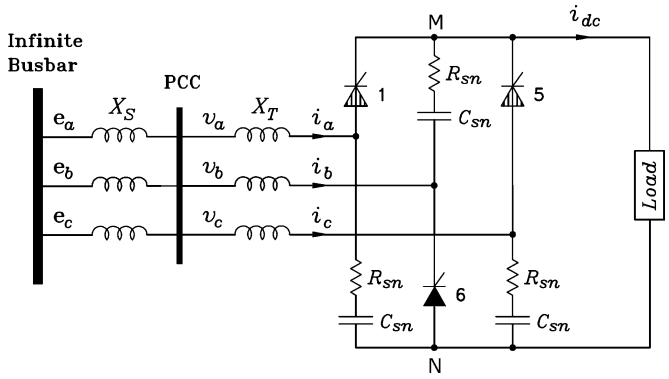

Fig. 4. Three-phase ac/dc converter during first conduction period with snubber circuits.

is clear that the snubber circuits of the ON-switches (1, 5, and 6) play no role in this analysis because of a short circuit in their two ends. Only the snubber circuits of the OFF-switches (2, 3, and 4) should be considered. By simplifying the converter circuit in Fig. 4, the equivalent circuit shown in Fig. 5 is achieved.

The differential equation of this figure can be simply achieved as a function of phase "b" current, as follows:

$$\frac{d^2 i_{\rm b}(t)}{dt^2} + \frac{2R_{\rm eq}}{3L_{\rm c}}\frac{di_{\rm b}(t)}{dt} + \frac{2i_{\rm b}(t)}{3L_{\rm c}C_{\rm eq}} = -\frac{\omega}{L_{\rm c}}V_m \,{\rm Cos}\left(\omega t + \frac{\pi}{3}\right) - \frac{2i_{\rm dc}}{3L_{\rm c}C_{\rm eq}} \tag{6}$$

where $R_{\rm eq} = R_{\rm sn}/3$, $C_{\rm eq} = 3C_{\rm sn}$, and $X_C = X_S + X_T$. Additionally, $R_{\rm sn}$ and $C_{\rm sn}$ are the resistance and the capacitor of snubber circuits, respectively.

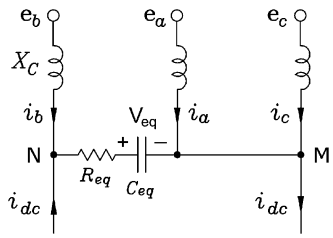

Fig. 5. Equivalent circuit of the converter in the first conduction period.

When $i_{\rm dc}$ is smooth, the current of phase b and its derivative at $t_o = \alpha + \pi/6$ are calculated as follows:

$$i_{\rm b}(t) = \left[V_C^{(1)}(t) - \exp\left(\frac{-(t-t_o)}{\tau_{\rm ci}}\right)\left[\left(V_C^{(1)}(t) + \frac{2i_{\rm dc}}{3L_cC_{\rm eq}}\right) \times \cosh\left(\omega_{\rm ci}(t-t_o)\right) + \frac{1}{2\omega_{\rm ci}}\left(\frac{2R_{\rm eq}}{3L_{\rm c}}V_C^{(1)}(t) - \frac{4\dot{i}_{\rm b}(t_o)}{3L_{\rm c}C_{\rm eq}}\right)\sinh\left(\omega_{\rm ci}(t-t_o)\right)\right]\right]\frac{3L_{\rm c}C_{\rm eq}}{2} \tag{7}$$

where

$$V_C^{(1)}(t) = -\frac{\omega V_m}{2L_{\rm c}C_{\rm eq}}\cos(\omega t) + \frac{\sqrt{3}\omega V_m}{2L_{\rm c}C_{\rm eq}}\sin(\omega t) - \frac{2i_{\rm dc}}{3L_{\rm c}C_{\rm eq}}$$

$$\omega_{\rm ci} = \frac{1}{2L_{\rm c}}\sqrt{\frac{8L_{\rm c}}{3C_{\rm eq}} - \frac{4R_{\rm eq}^2}{9}} \quad \tau_{\rm ci} = \frac{3L_{\rm c}}{R_{\rm eq}} \quad t_o = \alpha + \frac{\pi}{6}$$

$$\dot{i}_{\rm b}(t_o) = \frac{di_{\rm b}(t_o)}{dt} = \frac{2V_m}{3L_{\rm c}}\left[\frac{\sqrt{3}}{6}\sin(\alpha) - 3\cos(\alpha)\right]. \tag{8}$$

If the inequality $(4R_{\rm eq}^2/9 < 8L_{\rm c}/3C_{\rm eq})$ was true, then the current of phase "b" would contain oscillations with angular frequencies $(\omega_{\rm ci})$. The current oscillations in the feeder lines of the converter create oscillations in the converter bus and the PCC voltages in the commutation process. The damping time-constant of current oscillations $(\tau_{\rm ci})$ depends on $L_{\rm c}$ and $R_{\rm eq}$. A higher value of X_C or a lower value of $R_{\rm eq}$ increases the damping time of oscillations, which arises from the voltage notch.

Similarly, in order to analyze the equivalent circuit of the converter after the commutation period, the frequency $(\omega_{\rm co})$ and the damping time-constant $(\tau_{\rm co})$ of the oscillations on the voltage and current waveform are discovered by

$$\omega_{\rm co} = \frac{1}{6L_{\rm c}}\sqrt{\frac{36L_{\rm c}}{C_{\rm eq}} - 9R_{\rm eq}^2} \qquad \tau_{\rm co} = \frac{2L_{\rm c}}{R_{\rm eq}}\theta. \tag{9}$$

The voltage notch depth in the first conduction period, with the mentioned assumptions in this status, can be obtained as follows:

$$V_{\rm dep(b)} = \frac{X_S}{3(X_S + X_T)}V_m\left[\frac{\sqrt{3}}{3}\cos\left(\omega t + \frac{\pi}{3}\right)\right]_{\omega t = \alpha + \pi/6}. \tag{10}$$

The voltage notch depth $(V_{\rm dep})$ is an instantaneous variation of the voltage magnitude at the beginning of the

TABLE III
SYSTEM SPECIFICATIONS FOR NOTCH ANALYSIS USING SNUBBER CIRCUITS

Parameter	Value	Parameter	Value
$e_{(a,b,c)}$	220 V_{rms}	$R_{S(a,b,c)}$	$\approx 0\ \Omega$
f_s	50 Hz	$X_{S(a,b,c)}$	0.942 Ω
α	30 degree	$X_{T(a,b,c)}$	0.942 Ω
R_{sn}	200 Ω	R_L	10 Ω
C_{sn}	0.05 μF	L_L	2 H

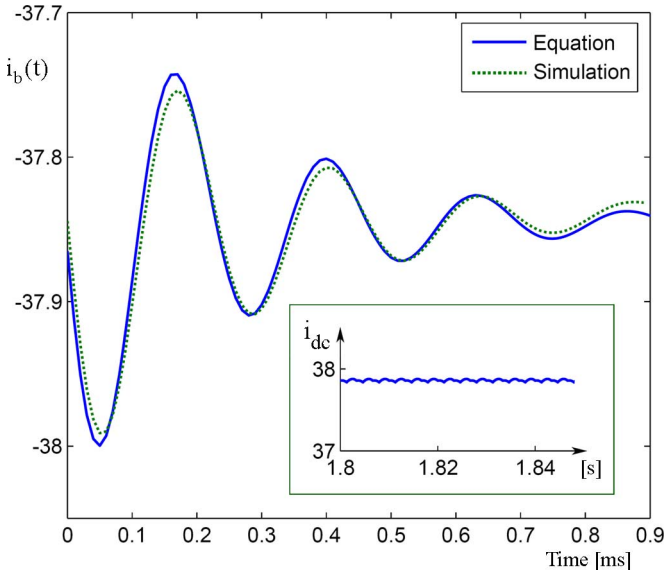

Fig. 6. $i_b(t)$ waveforms at the commutation time when i_{dc} is smooth.

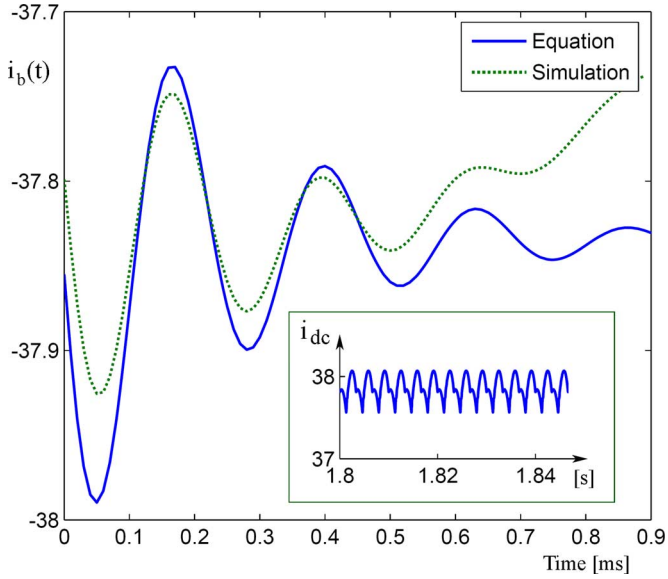

Fig. 7. $i_b(t)$ waveforms at the commutation time when i_{dc} is not smooth.

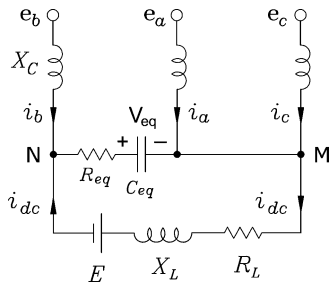

Fig. 8. Simplified equivalent circuit of the converter during the first conduction period with *RLE* load.

commutation period. The positive and negative values of the notch depth (V_{dep}), calculated from (5) or (10), refer to overshoots and undershoots on the converter voltage waveform, respectively.

In general, in all analytical states, the voltage notch depth depends on $X_S/(X_S + X_T)$. This means that a higher value of X_S/X_T increases the notch depth in PCC voltages. Therefore, in a weak system (with a lower short-circuit level or high system impedance), the voltage notch becomes deeper. To verify the validity of obtained relations, an ac/dc converter is simulated by the parameters value that is noted in Table III.

The dc current ripple factor $(K_{id} = (i_{dc(max)} - i_{dc(min)})/2i_{dc(avg)})$ suitably shows the smoothness of the current. A sufficiently large inductor load value of the converter is chosen so that the assumption of the smoothness of the dc current can be obtained. In this case, K_{id} is calculated to be 0.001. The obtained results for the current of phase b are compared with those from (7) in Fig. 6. This figure reveals that the results overlap with one another, which is proper. Interestingly, the oscillation frequencies are equal in both manners. Obviously, the frequency of these oscillations (f_{ci}) by simulation is approximately 4300 Hz; by (8), it is calculated to be 4291 Hz.

Increasing $8L_C/3C_{eq}$ causes the converter current to shift to oscillatory mode during commutation time, which affects the converter's ac voltage. Hence, the higher system impedance and the lower snubber circuit capacitance push the converter toward an oscillatory status in the commutation period. Equations (8)–(10) are true only when considering the smoothness of the dc line current (i_{dc}); whenever this current is not smooth, these equations cannot be reliable. If the inductance value of the converter load decreases to 0.15 H ($K_{id} = 0.013$), then the dc line current will not be smooth; consequently, analytical and simulation results are not compatible (see Fig. 7). This matter mentions that this method is suitable for application in current-source converters, and that the ripple of dc current must be considered in general ac/dc converters.

IV. IMPACT OF DC CURRENT RIPPLE ON THE NOTCH

For an applicable analysis of the voltage notch, it is necessary to consider the nonsmoothness of the dc line current. The ripple size of the dc current depends on the inductance value of the dc load and the smoothing reactor of the converter. *RLE* loads include a wide range of ac/dc converter loads; therefore, in this analysis, the RLE load is chosen in order to study the voltage notch, considering the nonsmoothness of the dc line current. Because of the load, the simplified equivalent circuit of the converter during the first conduction period is shown in Fig. 8.

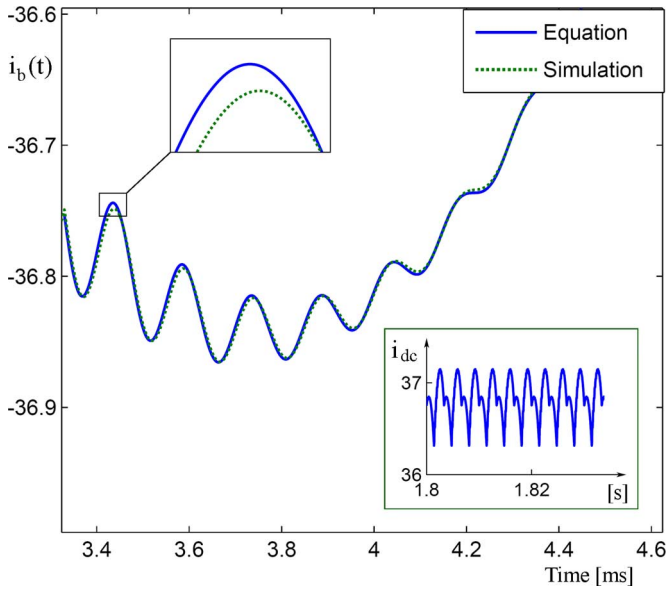

Fig. 9. $i_{\rm b}(t)$ waveforms at the commutation time when $i_{\rm dc}$ is not smooth.

Solving differential equations of the voltages and currents for this equivalent circuit requires long and complex equations for converter ac currents. In this case, to achieve the converter ac currents, the frequency domain equations are used in the manner as follows (11), shown at the bottom of the page, where

$$F(s)=\left(\sqrt{3}V_m\left(\frac{s-\sqrt{3}\omega}{2\left(s^2+\omega^2\right)}\right)+L_{\rm c}i_{\rm dc}(t_o)\right)$$
$$Z_L=R_L+sL_L$$
$$G(s)=\left(\sqrt{3}V_m\left(\frac{s+\sqrt{3}\omega}{2\left(s^2+\omega^2\right)}\right)+L_{\rm c}i_{\rm dc}(t_o)\right)$$
$$Z_{\rm eq}=R_{\rm eq}+\frac{1}{sC_{\rm eq}}$$
$$K(s)=\left(-\frac{\sqrt{3}V_m\omega}{s^2+\omega^2}-\frac{E}{s}+\left(2L_{\rm c}+L_L\right)i_{\rm dc}(t_o)\right). \quad (12)$$

This complicated relation in the frequency domain involves longer and more sophisticated relations in the time domain or else its presentation will not be useful. Numerical solutions can help solve this problem. With this method, the results of the aforementioned equations can be compared with the characteristics obtained from the simulation depicted in Fig. 9. Precise compatibility of these two characteristics indicates the accuracy of the analysis process at the commutation time by considering the dc current ripple ($K_{\rm id}=0.024$).

In this case, it is necessary to know the dependency of the oscillations' frequency and their existence condition as a relation. This is possible when the natural frequencies of the network are known. Fig. 10 shows the dead equivalent circuit of the converter at the first conduction period with its system impedances from the viewpoint of the switch that turns ON at the beginning of this conduction period. This equivalent circuit indicates the natural frequencies of the system, which are excited by voltage notches. For example, the transfer function of the phase "b" current, which is excited by the voltage notch ($V_{\rm dep}$), has the following form:

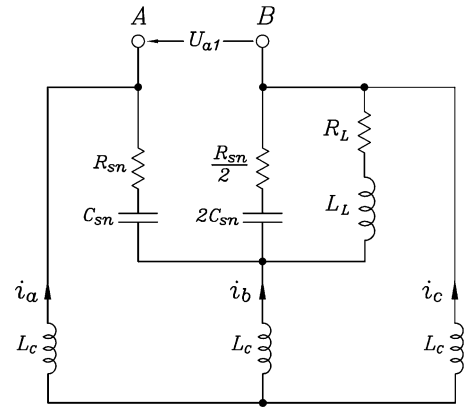

Fig. 10. Dead equivalent circuit seen from two ends of the switch T_1.

$$H(s)=\frac{I_{\rm b}(s)}{V_{\rm dep}(s)}=\frac{C_{\rm sn}L_Ls^2+(R_{\rm sn}C_{\rm sn}L_{\rm c}+R_{\rm sn}C_{\rm sn})s+1}{a_3s^3+a_2s^2+a_1s+a_0}$$
$$a_0=2R_L \qquad a_1=3L_{\rm c}+2R_{\rm sn}R_LC_{\rm sn}+2L_L$$
$$a_2=9R_LC_{\rm sn}L_{\rm c}+3R_{\rm sn}C_{\rm sn}L_{\rm c}+2R_{\rm sn}C_{\rm sn}L_L$$
$$a_3=9C_{\rm sn}L_{\rm c}L_L. \quad (13)$$

The natural frequencies of this equivalent circuit are the poles of transfer function (or the roots of characteristic equation) of (13), which are easily obtainable. In fact, if some of these poles were imaginary, then an oscillatory response during commutation would be expected, and the frequency of the oscillations would be determined from the imaginary portion of such poles. The aforementioned characteristic equation for a converter with the specifications detailed in Table III is concluded: $s^3+7445.7s^2+7.44\times10^8s+3.7\times10^9=0$.

The roots of this equation are $s_1=-4.97, s_{2,3}=-3720.36\pm27020.77j$, and the frequency of oscillations for the current of the converter is: $f_{\rm ci}=27020.77/2\pi=4300.5$. This frequency is identical to the previous value that was obtained from the simulation and (8).

V. Effects of System Capacitive Elements on the Voltage Notch

In the process of notch analysis, the power factor correction capacitors are considered, in addition to the snubber circuits and

$$I_{\rm b}(s)=\frac{-2Z_LG(s)+(R_{\rm eq}-Z_L)F(s)-2Z_{\rm eq}K(s)+\left(1/sC_{\rm eq}F^2(s)\right)}{(3L_{\rm c}Z_{\rm eq}+3L_{\rm c}Z_L)s+2Z_{\rm eq}Z_L} \quad (11)$$

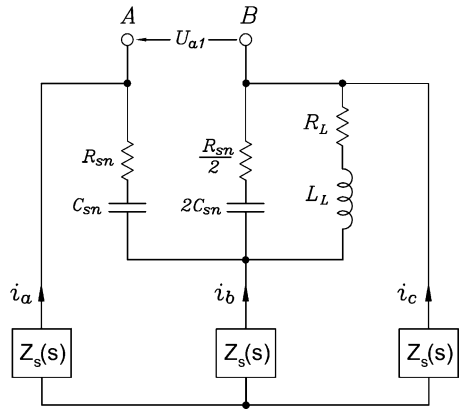

Fig. 11. Dead equivalent circuit seen from two ends of the switch T_1 with system impedance $Z_s(s)$.

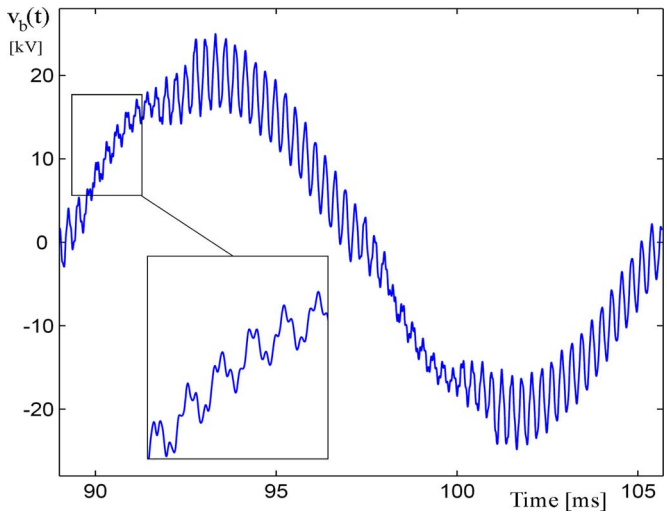

Fig. 12. Voltage waveform of the converter feeder supply.

the ripple of the dc current. The voltage notch in the network, which contains power factor correction capacitors or other capacitors like filters and the capacitive impedance of the cables, excites the natural frequencies of the network.

Because of the availability of the network structure, the characteristic impedance ($Z_S(s)$) that is seen from the converter bus can be drawn. Then, the frequencies that cause resonance can be clarified [8]–[11]. The number and value of oscillation frequencies, after the beginning of the commutation, depend on the imaginary poles of the transfer function of the system equivalent circuit. Fig. 11 illustrates this structure for the first conduction period with system impedance function $Z_s(s)$.

Fig. 12 shows the phase "b" voltage of an ac/dc converter, which is investigated in a system similar to a typical network that was used in [8]. The effects of the snubber circuits are also considered. Fig. 13 depicts the harmonic spectrum of such voltage shape; it is clearly observed that the existing oscillations in this characteristic originate from several frequencies. The 61th-order harmonic was noted in the aforementioned reference, and the 221th-order harmonic has a lesser amplitude.

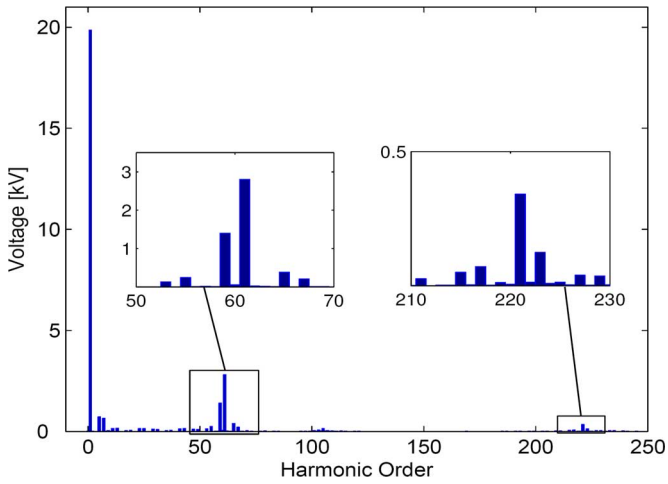

Fig. 13. Voltage harmonic spectrum related to the converter feeder supply.

TABLE IV
PARAMETERS OF THE EXPERIMENTAL SYSTEM

Parameter	Value	Parameter	Value
$e_{(a,b,c)}$	≈ 223 V_{rms}	$R_{S(a,b,c)}$	0.120 Ω
f_s	50 Hz	$X_{S(a,b,c)}$	0.077 Ω
α	different	$X_{T(a,b,c)}$	≈ 0 Ω
R_{sn}	60 Ω	R_L	25 Ω
C_{sn}	0.1 μF	L_L	0.8 H

Of course, by neglecting the effects of essential parameters of the converter (the load characteristic and snubber circuits), the other oscillatory frequencies of the voltage and the current waveforms can be achieved easily from the system frequency characteristic ($Z_s(S)$).

VI. EXPERIMENTAL RESULTS

For experimental investigation of the voltage notch at different conditions of the converter, several system parameters (such as system impedance, firing angle, and converter smoothing reactor) must be changed so that the analytical equations can be compared with the practical results. Therefore, a converter similar to the simulated system was considered, with the difference that the experimental system impedances were obtained from the system identification process [17], [18]. The parameters of the experimental system are presented in Table IV. The capacitor banks in the feeders of this system were so far away from the converter bus that the related effects on the voltage notch characteristic could be neglected.

Fig. 14 shows the voltage characteristic of phase "a" of this converter at a firing angle of 15°. The relatively low impedance of the system causes the notch width to narrow, and causes the oscillatory behavior of the voltage to rapidly damp. In this experiment, the system impedance is not great enough to allow observation of the performed analysis. Therefore, by adding impedance equal to $Z_{\rm add} = 0.122 + j0.945$ Ω in each phase, the experiments were repeated. The voltage waveform of the converter is shown in Fig. 15 at the firing angle of 30°.

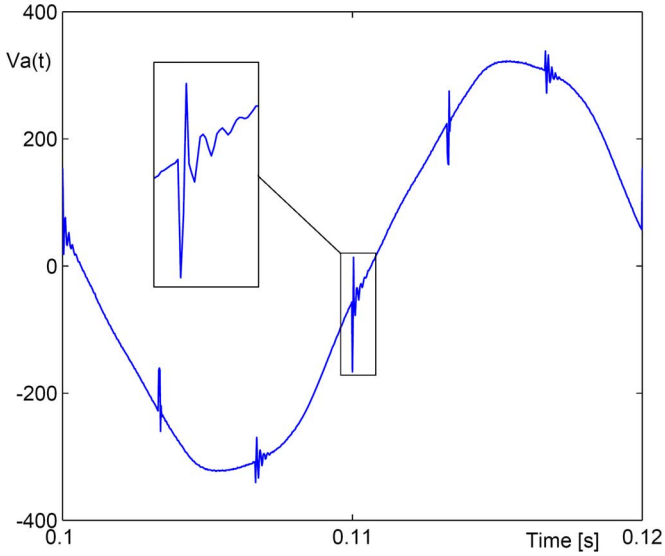

Fig. 14. Experimental voltage waveform of the converter (phase "a").

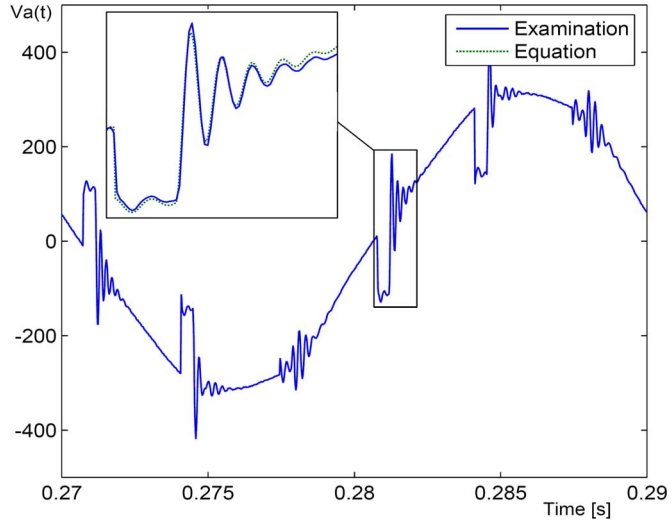

Fig. 16. Experimental voltage waveform with additional system impedances (by sampler circuit).

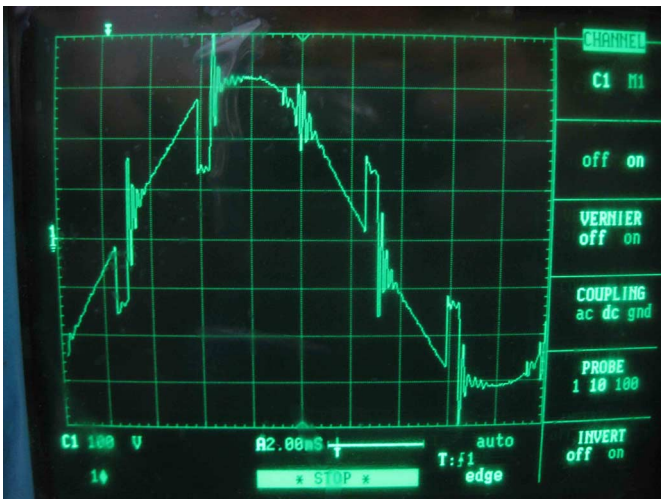

Fig. 15. Experimental voltage waveform with additional system impedances (by oscilloscope).

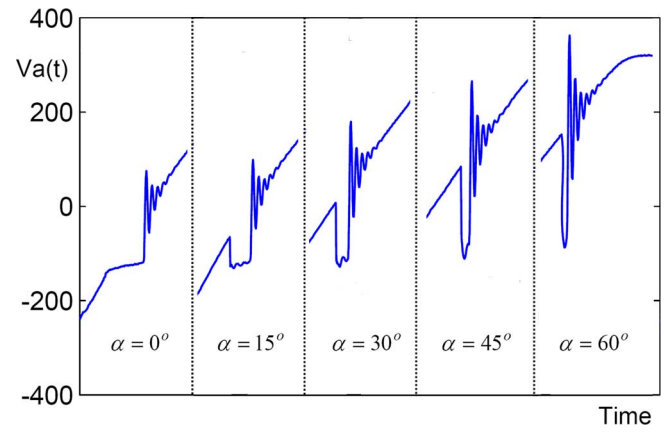

Fig. 17. Experimental voltage waveform at various firing angles.

To facilitate the comparison between the experimental and the theoretical results, a sampler circuit with a sampling frequency of 50 kHz was used in each channel in order to measure and store the voltage and the current characteristics of the converter. The results were transmitted to the MATLAB and plotted, as shown in Fig. 16. In this figure, one of the voltage notches is compared with the characteristic obtained from (11) and (12). The coincidence of these two characteristics confirms the effectiveness and accuracy of the presented theoretical relations. The frequencies of voltage oscillations in this practical waveform during and after the commutation period are nearly 4100 and 5000 Hz, and the corresponding values are calculated to be 4057 and 4961 Hz from (8) and (9), respectively.

Fig. 17 shows the experimental characteristics of voltage notch on the converter bus voltage with various firing angles by identical scale. This figure demonstrates notch depth dependency on the firing angle and the oscillations' frequency independency on the firing angle. As seen in this figure, the oscillations' magnitude, which is known as voltage overshoot, increases concurrently with the increase of the fire angle.

The type of converter load and the size of dc current ripples affect the characteristics of the voltage notches, and the load inductance (L_L) plays the most important role. Therefore, this inductance was removed from the converter load, and the experiments were repeated by resistive load. Fig. 18 compares two wave shapes that are related to the converter voltage with *R* and *RL* loads under similar conditions and at firing angles of 30°. This figure illustrates that decreasing load inductance has a noticeable impact on the more rapid damping of the voltage oscillations.

According to (8) and (9), the damping rates of voltage oscillations at and after the commutation periods depend on the snubber circuit resistance values in such a way that when this resistance increases, the generated oscillations are damped at higher rates. The obtained experimental results, shown in Fig. 19, confirm this fact.

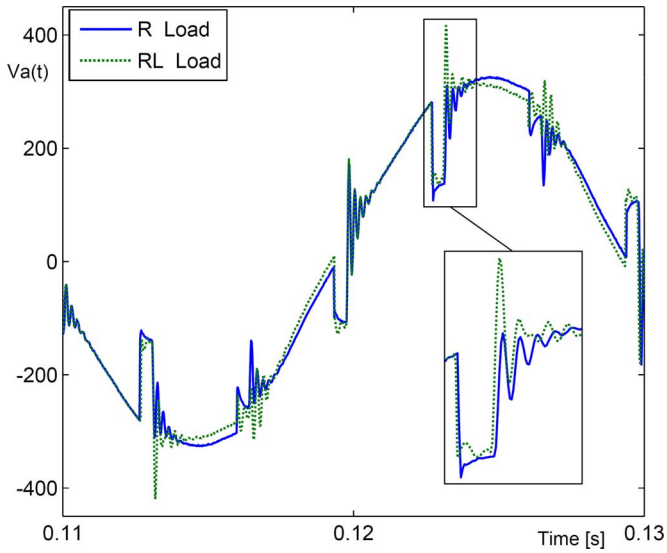

Fig. 18. Experimental voltage waveform with *R* and *RL* loads.

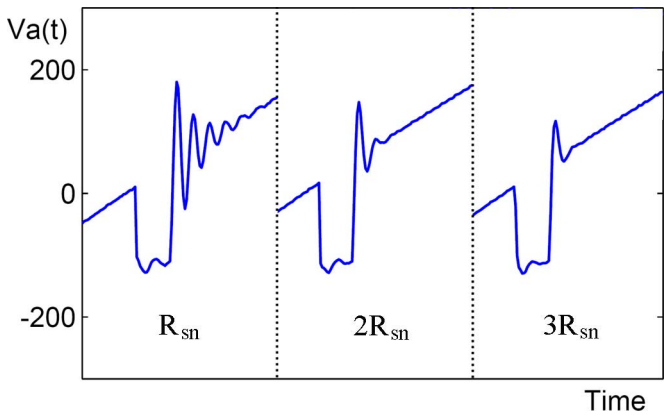

Fig. 19. Damping of the voltage oscillations by increasing snubber circuit resistance in the laboratory.

VII. Conclusion

This paper has analyzed the voltage notch problems that arise from the operation of the ac/dc converter, which is one of the most important disturbance sources in power systems. The analysis concentrated on the effects of the system and converter parameters on the voltage notch. This matter concerns large industrial consumers that have low short-circuit levels.

This paper investigated the effects of system impedances, capacitor banks, snubber circuits, firing angles, and types of converter loads on voltage notch characteristics. The proposed relations accurately predict the frequency of oscillations in the voltage and current waveforms of the converter bus that originate from voltage notch. In relation to the voltage notch, this study found that an increase in the system impedances causes the appearance of oscillations in the voltage of the converter bus, both during and after the commutation periods. Additionally, a decrease in the converter load inductance and an increase in the resistance of snubber circuits provide a more rapid damping rate for the oscillations. The simulation and the experimental results demonstrate the theoretical foundation, and the proposed equations are highly accurate and effective. The influences of various kinds of parameters on notch depth, frequency oscillations, and related damping have been investigated in the laboratory. This research will be useful in diagnosing power quality problems arising from ac/dc converter applications and in accurate harmonic analysis.

Subsequent efforts will endeavor to analyze the effects of the voltage notch on power networks, and to study the disturbances that arise from the voltage notch in buses that are near the converter bus.

References

[1] M. E. Villablanca, J. I. Nadal, and M. A. Bravo, "A 12-pulse AC–DC rectifier with high-quality input/output waveforms," *IEEE Trans. Power Electron.*, vol. 22, no. 5, pp. 1875–1881, Sep. 2007.

[2] B. Singh, S. Gairola, B. N. Singh, A. Chandra, and K. Al-Haddad, "Multipulse AC–DC converters for improving power quality: A review," *IEEE Trans. Power Electron.*, vol. 23, no. 1, pp. 260–281, Jan. 2008.

[3] V. A. Katic, J. M. Knezevic, and D. Graovac, "Application-oriented comparison of the methods for ac/dc converter harmonics analysis," *IEEE Trans. Ind. Electron.*, vol. 50, no. 6, pp. 1100–1108, Dec. 2003.

[4] Y. Sun, G. Zhang, W. Xu, and J. G. Mayordomo, "A harmonically coupled admittance matrix model for AC/DC converters," *IEEE Trans. Power Syst.*, vol. 22, no. 4, pp. 1574–1582, Nov. 2007.

[5] F. J. Chivite-Zabalza and A. J. Forsyth, "A passive 36-pulse AC–DC converter with inherent load balancing using combined harmonic voltage and current injection," *IEEE Trans. Power Electron.*, vol. 22, no. 3, pp. 1027–1035, May 2007.

[6] I. Sato, J. Itoh, H. Ohguchi, A. Odaka, and H. Mine, "An improvement method of matrix converter drives under input voltage disturbances," *IEEE Trans. Power Electron.*, vol. 22, no. 1, pp. 132–138, Jan. 2007.

[7] E. Ngandui, M. de Montigny, and P. Sicard, "Comparison of converter transfer function models for estimate harmonic currents generated by ac/dc converters under unbalanced conditions," in *Proc. IEEE Can. Conf. Electr. Comput. Eng. (CCECE 2003)*, May 4–7, vol. 1, pp. 491–495.

[8] L. Tang, M. McGranaghan, R. Ferraro, S. Morganson, and B. Hunt, "Voltage notching interaction caused by large adjustable speed drives on distribution systems with low short circuit capacities," *IEEE Trans. Power Del.*, vol. 11, no. 3, pp. 1444–1453, Jul. 1996.

[9] R. A. Adams, R. C. Catoe, J. G. Dalton, and S. G. Whisenant, "Power quality issues within modern industrial facilities," in *Proc. IEEE Annu. Textile, Fiber Film Ind. Tech. Conf.*, May 2–3, 1990, pp. 10/1–10/6.

[10] A. C. S. de Lima, H. W. Dommel, and R. M. Stephan, "Modeling adjustable-speed drives with long feeders," *IEEE Trans. Ind. Electron.*, vol. 47, no. 3, pp. 549–556, Jun. 2007.

[11] A. M. Gole, A. Keri, C. Kwankpa, E. W. Gunther, H. W. Dommel, I. Hassan, J. R. Marti, J. A. Martinez, K. G. Fehrle, L. Tang, M. F. McGranaghan, O. B. Nayak, P. F. Ribeiro, R. Iravani, and R. Lasseter, "Guidelines for modeling power electronics in electric power engineering applications," *IEEE Trans. Power Del.*, vol. 12, no. 1, pp. 505–514, Jan. 1997.

[12] B. C. Smith, N. R. Watson, A. R. Wood, and J. Arrillaga, "Steady state model of the AC/DC converter in the harmonic domain," *Inst. Electr. Eng. (IEE) Proc. Transmiss. Distrib.*, vol. 142, no. 2, pp. 109–118, Mar. 1995.

[13] R. Ghandehari, A. Shoulaie, and D. Habibinia, "The problems of voltage notch phenomena in power AC/DC converters," in *Proc. 42nd Int. Univ. Power Eng. Conf. (UPEC 2007)*, Sep. 4–6, pp. 992–996.

[14] D. D. Shipp and W. S. Vilcheck, "Power quality and line considerations for variable speed AC drives," *IEEE Trans. Ind. Appl.*, vol. 32, no. 2, pp. 403–410, Mar./Apr. 1996.

[15] C. K. Duffey and P. P. Stratford, "Update of harmonic standard IEEE-519: IEEE recommended practices and requirement for harmonic control in electric power systems," *IEEE Trans. Ind. Appl.*, vol. 25, no. 6, pp. 1025–1034, Nov. 1989.

[16] *IEEE Recommended Practices and Requirement for Harmonic Control in Electric Power Systems*, IEEE Group, IEEE Standard 519, 1992.

[17] G. Fusco, A. Losi, and M. Russo, "Constrained least squares methods for parameter tracking of power system steady-state equivalent circuits," *IEEE Trans. Power Del.*, vol. 15, no. 3, pp. 1073–1080, Jul. 2000.

[18] G. N. Bathurst, J. Arrillaga, N. R. Watson, and A. R. Wood, "Advanced modeling of the harmonic impedances of AC–DC converters," *Inst. Electr. Eng. (IEE) Transmiss. Distrib.*, vol. 149, pp. 700–704, Nov. 2002.

Reza Ghandehari (S'07) was born in Isfahan, Iran, in 1971. He received the B.Sc. and M.Sc. degrees in 1995 and 2002, respectively, from Iran University of Science and Technology (IUST), Tehran, Iran, where he is currently working toward the Ph.D. degree in electrical engineering.

He is with Tehran Regional Electrical Company (TREC). His current research interests include power electronics, power quality, electrical machine, and HVDC.

Abbas Shoulaie was born in Isfahan, Iran, in 1949. He received the B.Sc. degree from Iran University of Science and Technology (IUST), Tehran, Iran, in 1973, and the M.Sc. and Ph.D. degrees in electrical engineering from the Université des Sciences et Technologies de Lille 1 (U.S.T.L.), Montpellier, France, in 1981 and 1984, respectively.

He is currently a Professor of electrical engineering at IUST. His current research interests include power electronics, magnetic systems and linear motors, flexible alternating current transmission systems (FACTS) devices, and HVDC.